AD-A114 429 NAVAL OCEAN RESEARCH AND DEVELOPMENT ACTIVITY NSTL S--ETC F/G 8/3
MEASUREMENTS OF WHITECAP COVERAGE AND SURFACE WINDS OVER THE GU--ETC(U)
OCT 81 P M SMITH

UNCLASSIFIED NORDA-43 NL

END
DATE FILMED
6-82
DTIC

(10)

NORDA Report 43

Measurements of Whitecap Coverage and Surface Winds Over the Gulf of Mexico Loop Current

Peter M. Smith

Oceanography Division
Ocean Science and Technology Laboratory

October 1981

Distribution Unlimited

Naval Ocean Research and Development Activity
NSTL Station, Mississippi 39529

Foreword

With the advent of ocean scanning satellites such as SEASAT, the oceanographic community has been presented with data sets spanning mesoscale-wide swaths of ocean surface. Scientists tasked with evaluating the performance of satellite-borne microwave radiometers, for example, are faced with the challenge of determining the distribution of wind, sea surface temperature, centimeter scale waves, and whitecaps over these large areas of ocean surface. The work described herein is directed toward developing new techniques to synoptically survey such large areas of the ocean and provide the necessary surface truth with which to evaluate the new generation of all-weather satellite-borne sensors.

G.T. Phelps, Captain, USN
Commanding Officer
NORDA

Executive Summary

The fraction of the ocean surface covered by whitecaps has long been thought to be some monotonically increasing function of the prevailing wind velocity at least for large fetches. In order to determine the extent to which other factors such as air column stability or water mass type can influence the areal coverage of whitecaps, photographic data was collected over the Loop Current from a NAVOCEANO P-3 aircraft. The variation of whitecap coverage along a line of closely spaced (25 km) stations was determined and compared with other aircraft and data buoy information. The data indicates that, on the day of the flight, white-capping within the boundaries of the Loop Current depended little on the local wind, but demonstrated a noticeable dependence on air column stability. The strength and nature of this dependence varied over mesoscale distances. These results indicate that microwave radiometric measurements can be sensitive to variables other than surface wind since microwave brightness is quite sensitive to sea foam. The value of areal whitecap coverage as a measurable geophysical variable is also examined.

Acknowledgements

The author wishes to thank Dr. Vincent Cardone of Ocean Weather, Inc., for generously supplying the computer coding for the surface stress calculations and for the discussions concerning its use. I am also grateful to the crew of the NAVOCEANO aircraft, BIRDSEYE, and to Mr. Ed Arthur and Mr. John Schmidt of NORDA for the collection of the aircraft data.

Contents

Illustrations

Measurements of Whitecap Coverage and Surface Winds Over the Gulf of Mexico Loop Current

Background

Wave breaking and whitecapping is, at the same time, one of the more inspiring and one of the most important dynamical processes at work in the surface layers of the ocean. To the wave modeler, breaking represents a sink of wave energy; to the acoustic scientist, a source of noise energy; to the mixed layer modeler, a source of turbulence in the surface layer; and to the remote sensor, a bright source of microwaves. Yet, for all the importance of wave breaking, it is little understood and is seldom measured in the deep ocean.

Part of the difficulty of analyzing whitecaps stems from their intermittent character in both space and time. Since the areal coverage of whitecaps typically represents only about 1% of the sea surface, an image of the sea surface must encompass on the order of 500 m^2 in order to accumulate statistical samples of reasonably small (< 50% of the mean) standard deviation. Eulerian measurements suffer from a similar sampling problem. Longuet-Higgins and Smith (1981) reported that measurements made from a buoy during MARSEN indicated that on the average only one wave broke at the buoy during every 100 significant wave periods.

Photographic records of instantaneous areal whitecap coverage are the easiest whitecap data to obtain, and several investigators (Monahan, 1969; Monahan, 1971; Toba and Chaen, 1973; and Ross and Cardone, 1974) have attempted to relate whitecap coverage from photographs to measured wind stress and air column stability.

Most of this data shows considerable scatter when whitecap coverage is plotted against wind stress alone. However, Wu (1980) was able to reduce the scatter of Manahan's (1971) data by organizing the data according to the stability of the marine boundary layer. Apparently the air column stability affects the formation or lifetime of the bubbles that constitute the foam; however, no present theory can explain this apparent relationship. Another source of scatter is the lack of a well-defined whitecap boundary, as discussed in Blanchard (1971) and as demonstrated in Appendix A of this report.

In parallel to the field measurements of foam coverage, several investigators have made laboratory studies of bubble formation and stability as functions of the physics and chemistry of the water. Miyake and Abe (1948) measured the effects of salinity and temperature and found that for oceanic salinities, bubble stability was relatively insensitive to the small changes in salinity. Changes in temperature, on the other hand, had a marked effect on the persistence of bubbles. In particular, a 5° increase in temperature at 20°C produced a 5% decrease in bubble lifetime. Garrett (1967) studied the effects of surfactant concentrations on the stability of bubbles and found that small amounts of surfactants increase bubble stability, but concentrations in excess of one monomolecular thickness have the effect of shortening bubble lifetime. There have also been in situ measurements of bubble size distributions as a function of depth. Wu (1981) presents a summary of much of this work.

Theory

Monahan (1971) has proposed a functional form for the areal coverage of whitecaps,

$$W = A_o R_T^{\gamma} \qquad (1)$$

where W is the fractional coverage; A_o is the initial area generated by a breaking wave; R is the number of breaking waves occurring per unit area, per unit time; and τ is the mean lifetime of a whitecap. τ has been measured (Monahan and Zietlow, 1969) to be 1.54 seconds for fresh water and 3.85 seconds for salt water. Hence, the instantaneous whitecap coverage is a measure of the four-second time history of breaking as well as the instantaneous rate of breaking.

Wu (1979) reasoned that W should be proportional to the energy dissipation rate of breaking waves and arrived at a dependence of W on the wind speed:

$$W \sim u_*^3 \sim U_{10}^{3.75} \qquad (2)$$

where u_* is the friction velocity and U_{10} is the 10 meter wind speed. If the dependence of W on u_* in (2) is to hold, then the dependence of W on other variables such as air column stability or water temperature will likely appear as an additional factor:

$$W \sim u_*^3 f(s, T, \text{etc...}) \qquad (3)$$

where s is some measure of air column stability and T is water temperature. This functional form is suggested by equation (1) if one assumes that the u_* dependence resides in the product $A_o R$ and the other independent variables determine τ.

In this paper we describe an experiment designed to examine the dependence of whitecap coverage on atmospheric boundary layer stability over the ocean for the unstable regime. Whitecap statistics are measured at a series of 21 consecutive, colinear stations, each separated by 23 kilometers (km). The line of stations extends across the Gulf of Mexico Loop Current along a line of constant latitude. The results show that for slightly unstable boundary layers, the coverage appears to decrease as the layer becomes more unstable in agreement with Monahan (1971) and Wu (1980). However, for extremely unstable cases the whitecap coverage can either increase or decrease with stability, depending on the locale. The whitecaps measured were generated in the environment of a strong current and, hence, may not be representative of more benign areas of the ocean.

The Experiment

An instrumented NAVOCEANO P-3 aircraft was flown over the Loop Current in a westerly direction along the 26°N latitudinal line as shown in Figure 1. Data were collected from 1500Z to 1600Z on 2/8/80. The following instruments were used to collect data.

PRT-5 Radiation Thermometer (SST)
Thermal Infrared Scanner (SST)
Hasselblad Camera (Whitecaps)
Laser Surface Profiler (Sea State)
Wind Anemometer (Wind speed/direction)
Air Temperature Sensor (Air temperature)
Expendable BT's (Water Temperature Profiles)

The flight altitude was 670 meters (m) from 86°W to 88°W and 335 m for the remainder of the track. Aircraft speed was 125 meters per second (m/sec).

Two NOAA Data Buoy Office (NDBO) data buoys were located at 26°N,86°W (2003) and 25.9°N,89.6°W (2001), respectively, as shown in Figure 1. The buoys supply hourly reports of five meter height, three-minute-averaged wind speed and direction, air temperature, water temperature, and barometric pressure. These two buoys were the principle source of surface truth data for this experiment.

On 8 February 1980 the Loop Current flowed northward to the vicinity of 26°N, and then south and eastward into the Florida Straits. Figure 2 is a GOES infrared image of the Loop Current obtained at 0600Z on 7 February 1980 that shows the warm core of the Loop, the cooler slope water to the north and the east and a warm core anticyclonic eddy to the northwest. The sea surface temperature as determined by the airborne PRT-5, and verified by the buoy reports, is shown plotted in Figure 3.

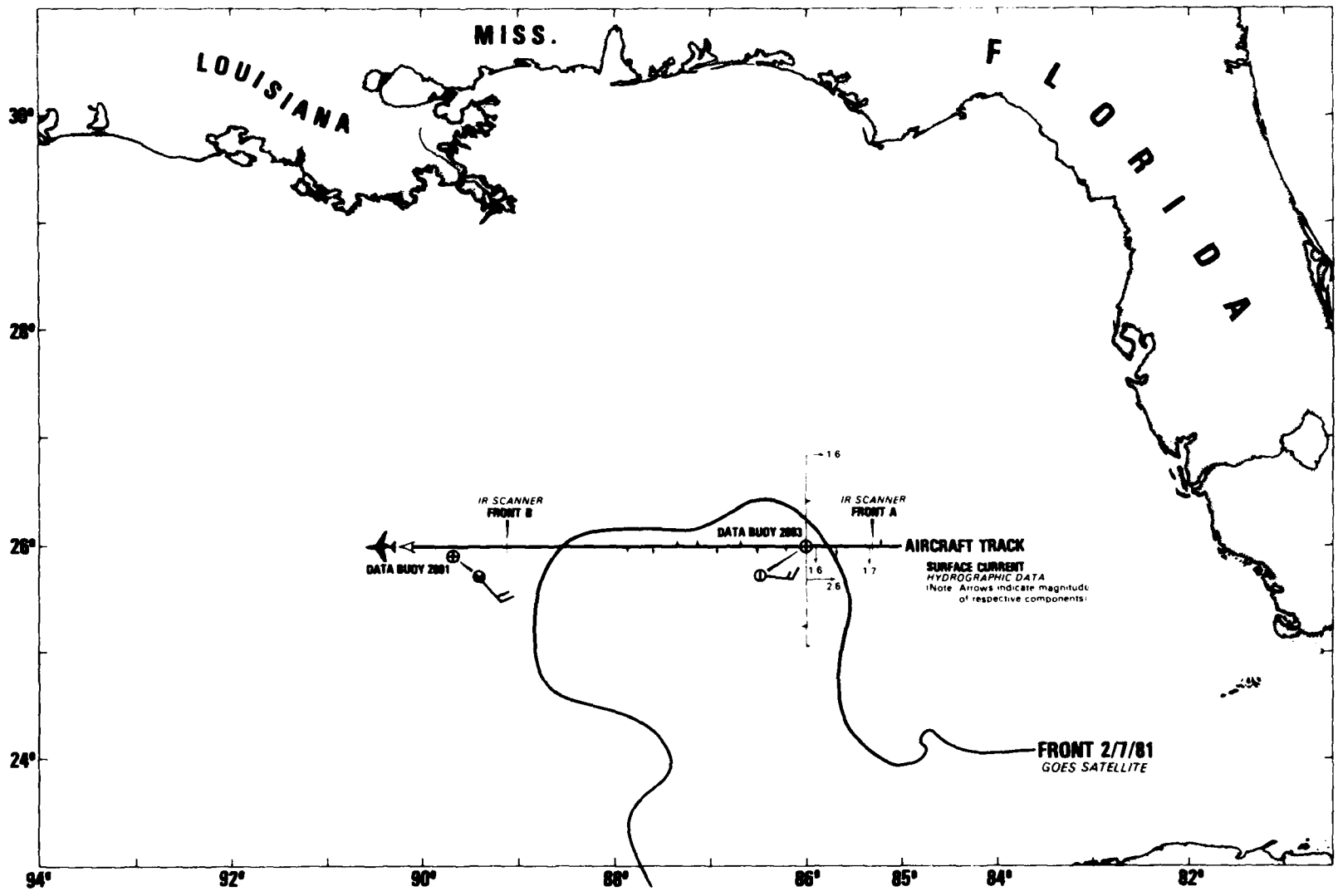

Figure 1. Gulf of Mexico aircraft track with surface current components

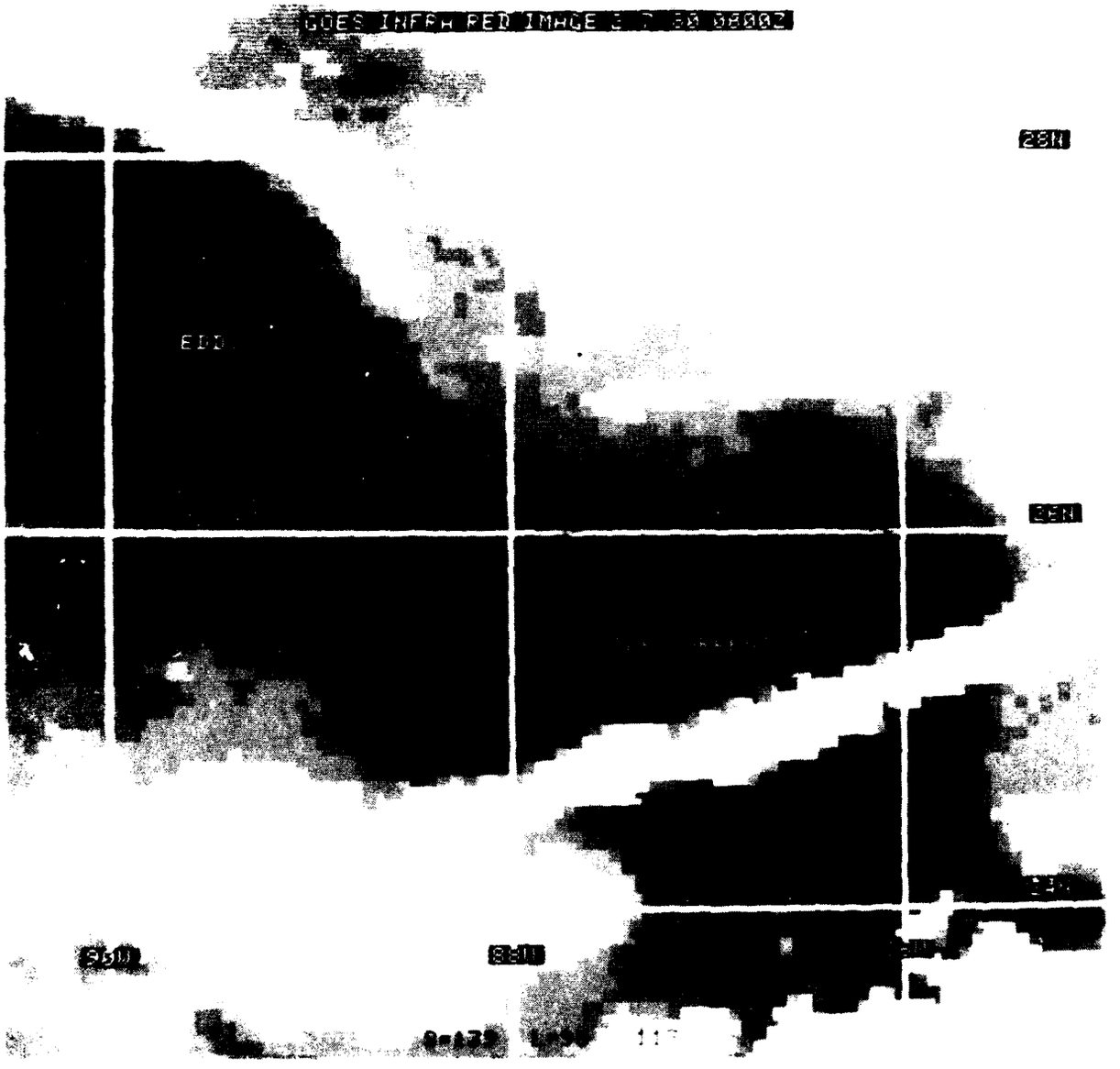

Figure 2 GOES Image of the Loop Current

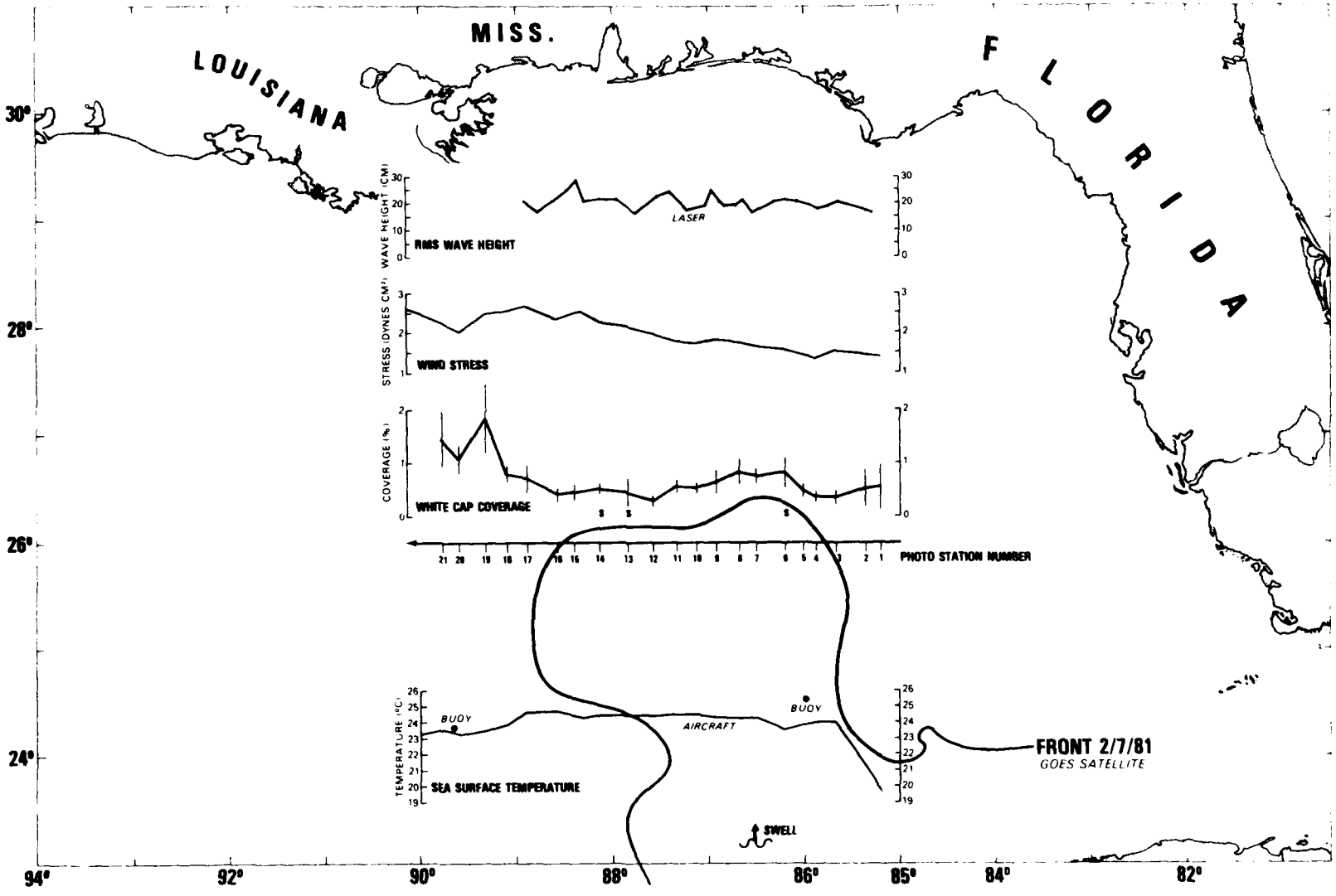

Figure 3. Plots of sea surface temperature, whitecap coverage, surface wind stress, and RMS waveheight vs. longitude

The sea surface temperature difference between the Loop and the Florida shelf water is seen to be approximately 5°C and approximately 1.5°C between the Loop and the eddy.

The infrared scanner mounted in the aircraft detected two fronts--the eastern front of the Loop Current and the western front of the Loop Current/ eastern front of the eddy (Fig. 4).

(1977). A reference depth of 350 m was chosen, and the resulting surface velocity components are shown as arrows along the aircraft track in Figure 1. Similarly, the E-W components were derived along the 86° meridian and are also shown in Figure 1. These estimated values for the surface current were later used to adjust the air-sea velocity shear for the calculation of surface wind stress.

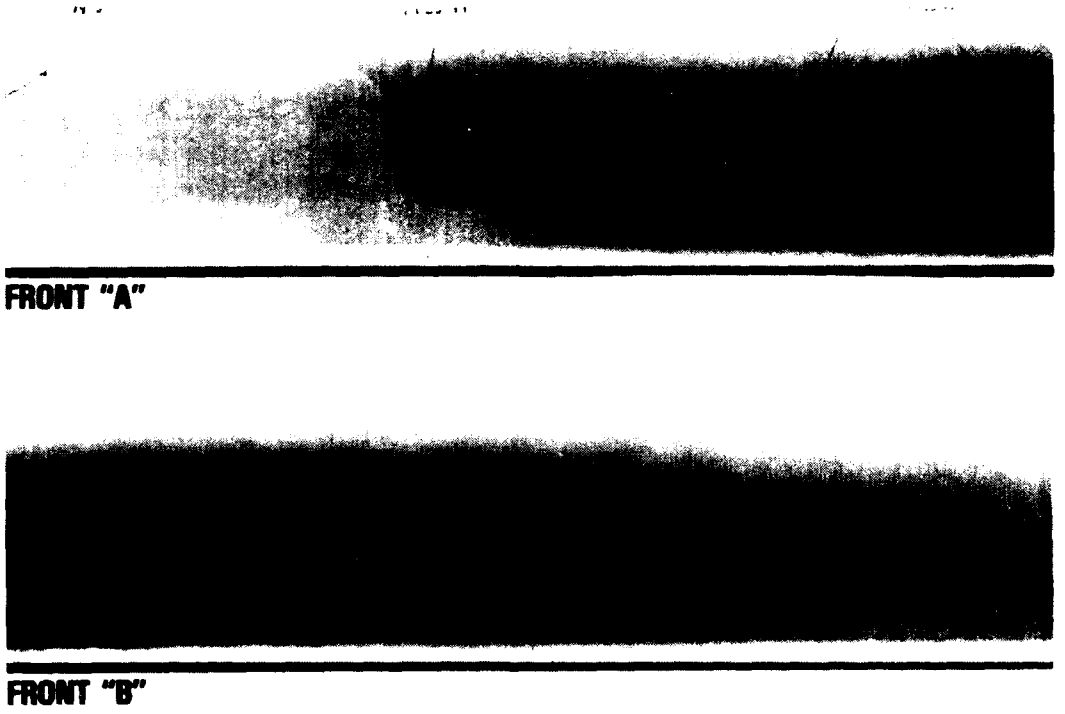

Figure 4. Infrared scanner images of loop current thermal fronts

These frontal boundaries agree with the fronts visible on the satellite image (Fig. 2).

The hydrographic data derived from AXBTs (Fig. 5) shows strong frontal characteristics to the north and the east of the Loop Current but weak gradients to the west. The N-S components of surface velocity along the track were estimated from the expendable bathythermograph (XBT) data and the temperature-salinity (T-S) characteristics of the Florida Current reported by Brooks and Niiler

Whitecaps were recorded on infrared sensitive film (Kodak 2424) and were later digitized into a 512x512 array on an image processing system. Ten images were recorded at each of the 21 photo stations. The usable field of view (FOV) of each photo was 370 m x 560 m up to station 15 and 185 m x 280 m for the remainder of the track, resulting in a pixel size of 1 m x 1 m. The image plane of the camera was not motion compensated and, hence, the minimum ground distance resolvable was one meter

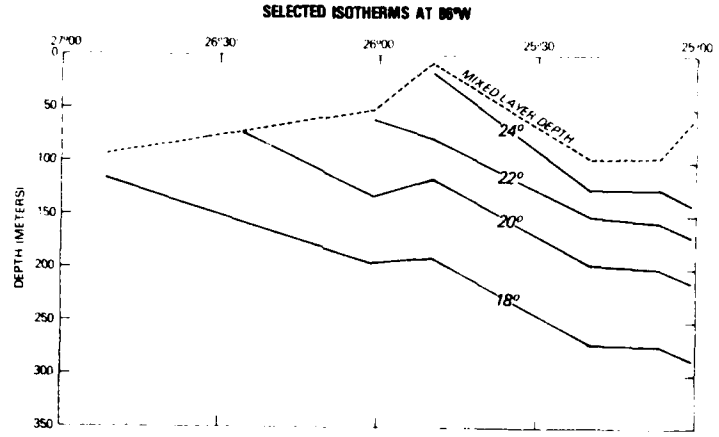

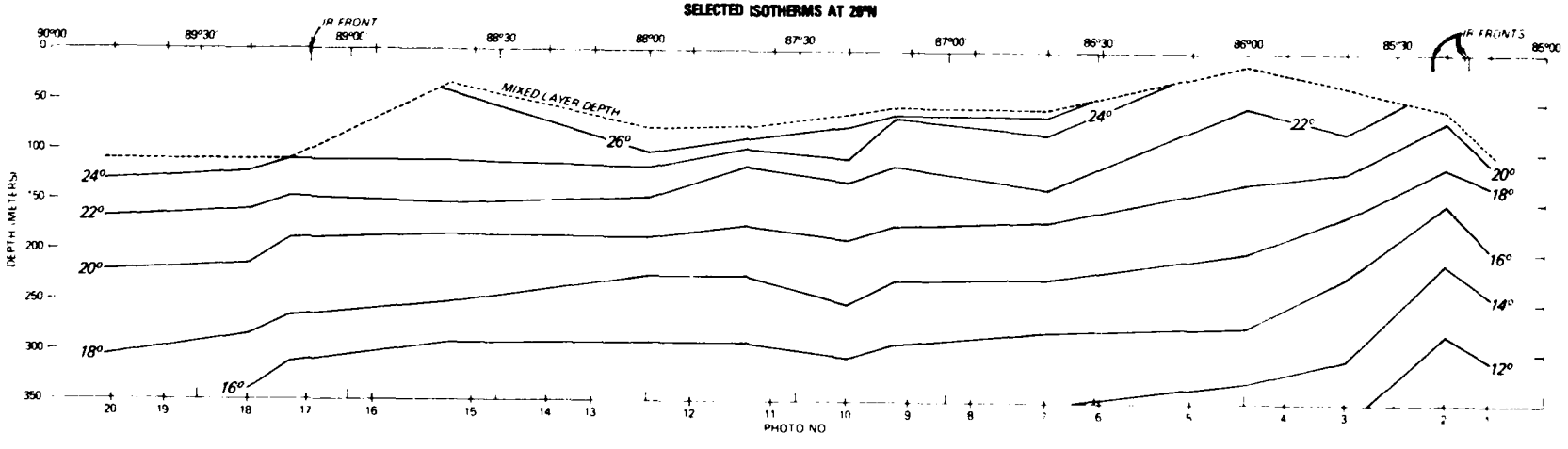

Figure 5. Hydrography

because of motion blurring. Twelve of the 210 images are shown in Figure 6. Streaks running north-south were evident in a few of the photos. One such photo is part of the station 12 series shown. Photos containing streaks were not included in the compilation of percentage whitecap coverage. The changes in whitecap coverage from station to station are considerable and, as can be seen from Figure 6, should be apparent to the most casual observer.

The digitized images were normalized by accomplishing an intensity stretching, area by area, in order to compensate for uneven lighting distributions. In the event that a cloud had obviously obscured the sun, the photo was discarded.

Areas of each image that appear bright enough to be whitecaps are "blotched" or saved on a one-dimensional "graphics plane" (1 x 512 array). The blotched areas are then divided by the total area considered to obtain the fractional whitecap coverage. In the present case all pixels with an intensity value greater than 160 on a 0-256 scale were blotched. An error analysis of this somewhat subjective process appears in Appendix A. The uncertainty resulting from such an analysis is estimated from Figure A-3 to be approximately $\pm$0.25% coverage. Care was taken to assure that digitizing conditions were identical for all 210 images.

The mean percentage whitecap coverage of each group of images was calculated, and the results are plotted in Figure 3 as a function of longitude. The standard deviation is shown by the length of the vertical line drawn at each station. Many images, especially near the western end, were affected by clouds and could not be used. As a result some station means are based on as few as three (e.g., station 19) samples.

Surface Wind Stress

The computer program, PROPAR, developed by Cardone and reported in Cardone (1969) was used to infer the wind stress from 5 m wind velocities, sea surface temperature, air temperature, barometric pressure, and an estimated relative humidity. The 5 m winds present at stations between the data buoys were obtained by fitting the aircraft-measured wind speed to the 5 m winds measured at the buoys. This amounts to assuming that the effect of the higher altitude is to scale up the wind velocities by some constant factor between the buoys. Sea surface temperature was measured from the aircraft using the IR radiometer. Since the IR-derived temperatures at the buoys were approximately 0.5°C lower than the in situ temperatures measured by the buoy sensors, they were assumed to be correct.

Air temperatures measured at altitude were reduced to the surface by using the buoy-measured values as calibration points in the same manner as the wind speed. It was noted that the temperature lapse rate was higher than the adiabatic lapse rate in the boundary layer and lower at altitude.

Barometric pressure was linearly interpolated between the buoys. The relative humidity was not available from the buoys at the time, however, buoys presently instrumented are reporting between 50 and 100% R.H. A value of 70% was assumed.

Surface wind velocities were adjusted for the estimated surface current. The surface current was determined through a combination of the surface current components derived from the measured hydrography and the pattern of surface isotherms. The resulting wind stress is shown plotted against longitude in Figure 3. The wind stress is directed toward the west and northwest and increases monotonically from east to west, primarily as a result of the increasing wind speed (the 5 m wind increases from 8 m/sec at the east end to 10 m/sec at the west end).

Sea State

The sea state was characterized by an energetic swell propagating from the south combined with shorter wind waves

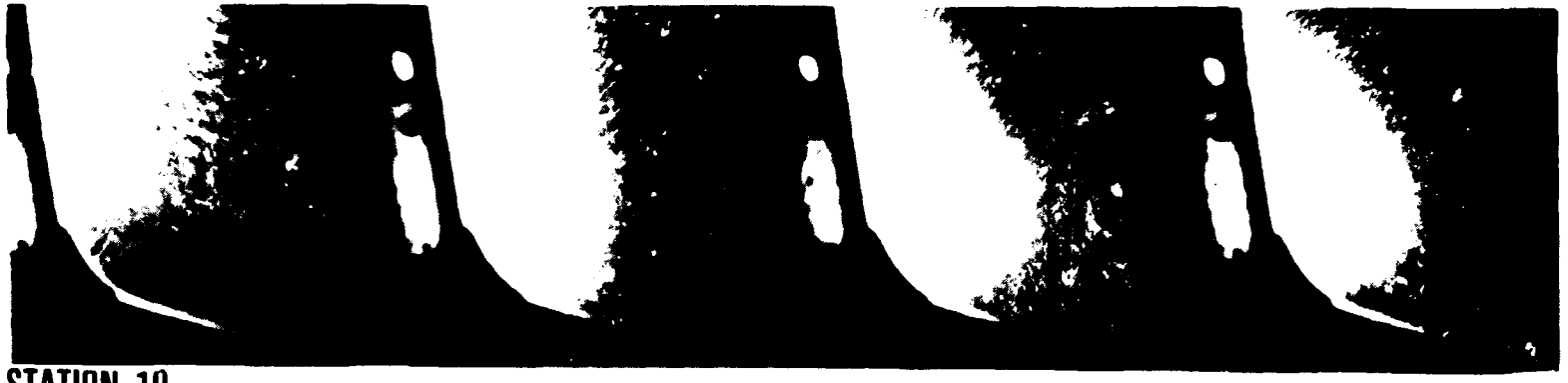

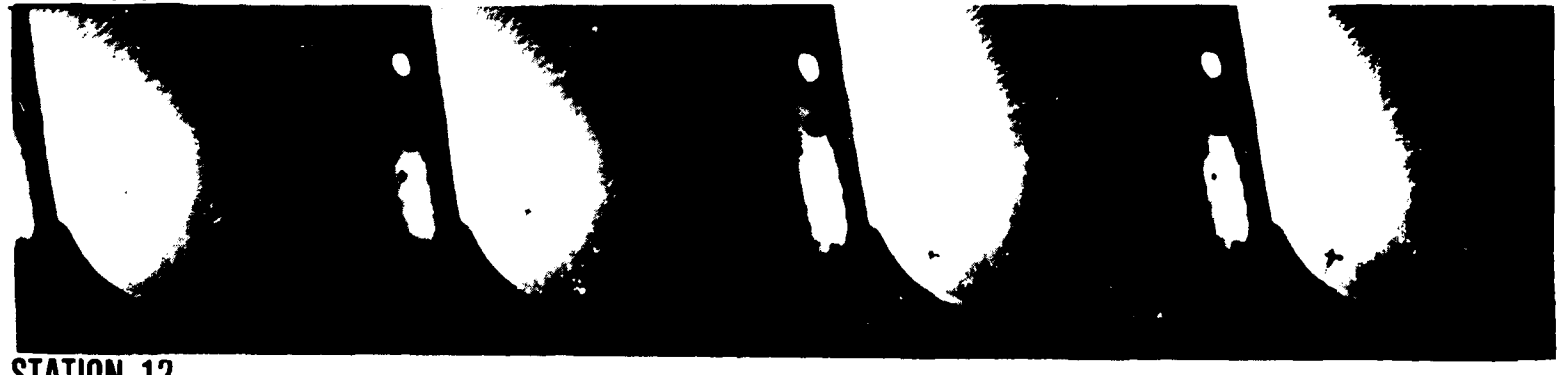

Figure 6. Sample images

aligned with the westerly wind direction. Evidence of both wave fields could be seen in a Fourier-transformed photographic image of the sea surface. Figure 7 shows the wave height power spectra measured at the two NDBO data buoys. The swell period of 6.25 seconds can be seen in both spectra. The TV video record of the sea surface shows the whitecaps breaking toward the north, indicating that the northward-propagating swell was the dominant contributor to the observed foam. Since the wind turned from westerly at the east end of the flight line to northwesterly at the west end, the increase in swell amplitude and resulting whitecapping toward the west can be explained by the interaction of the northward-propagating swell with the more favorable northwesterly wind in evidence at buoy 2001.

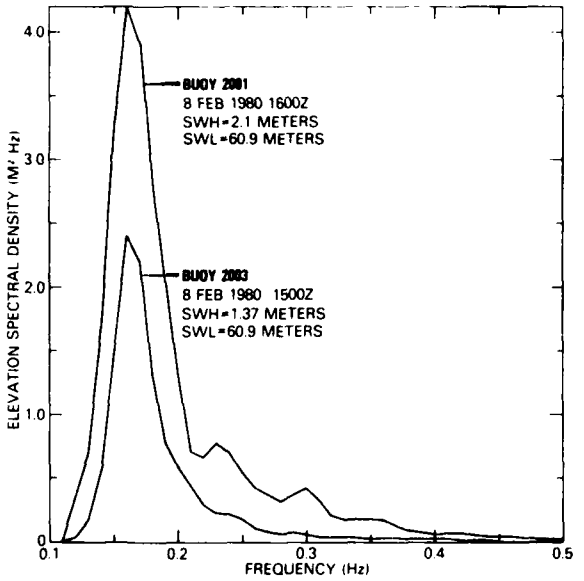

Figure 7. Wave height spectra at NOAA data buoys 2001 and 2003

The laser profiler on the P-3 records wave height as a function of along-track distance. Due to periodic noise spikes in the data, the typical continuous wave height record length was of order 3 km. The profiles were digitized and root-mean-square wave height computed. The results are shown plotted against longitude in Figure 3. No systematic increase in significant wave height appears from east to west; however, the laser records did not extend far enough to the west to reflect the corresponding increase in the whitecap coverage at the west end of the flight line.

The whitecap, friction velocity, and air-sea temperature difference data are compiled in Table I.

TABLE I

Station No.	Whitecap Coverage (%)	Standard Deviation	ΔT	No. of Photos Analyzed
1	0.57	0.34	-1.25	6
2	0.55	0.29	-2.90	10
3	0.35	0.13	-5.15	8
4	0.37	0.08	-4.65	10
5	0.48	0.11	-3.85	6
6	0.83	0.23	-4.30	7
7	0.74	0.13	-3.65	10
8	0.82	0.19	-3.40	9
9	0.66	0.18	-3.65	8
10	0.54	0.07	-3.25	10
11	0.59	0.09	-3.05	9
12	0.30	0.07	-3.10	9
13	0.46	0.19	-3.40	7
14	0.54	0.08	-2.80	9
15	0.47	0.12	-3.30	9
16	0.41	0.11	-3.15	8
17	0.73	0.22	-2.20	9
18	0.84	0.11	-1.55	4
19	1.89	0.50	-1.35	3
20	1.06	0.22	-1.65	7
21	1.46	0.42	-1.50	7

Discussion

The whitecap coverage shown in Figure 3 appears to be a smoothly varying function of space, at least in the region of the Loop Current. Since the standard deviation of each estimate is well below the mean, the fluctuations are believed to be geophysical rather than a result of statistical uncertainties. The most striking property of the whitecap coverage is its weak dependence on the surface wind stress. Whereas the wind stress gradually increases from east to west, the whitecap coverage exhibits a somewhat wind-independent behavior. Also, coverage appears to be generally lower within the Loop Current than to the west. A dependence of whitecap

coverage on influences other than the wind is suggested. A marked decrease in whitecap coverage occurs in the vicinity of both Loop Current fronts. A similar decrease in coverage was observed by Ross and Cardone (1974) near the north "wall" of the Gulf Stream.

Whitecap coverage is plotted with the air-sea temperature difference as an indicator of air column stability in Figure 8. A definite correlation appears to exist. In order to remove the wind stress dependency of the whitecap coverage, W, and to make the dependence of W on stability more explicit, we scale the whitecap coverage by u_*^3 as suggested by equation (3), and plot this scaled W against ΔT. The resulting plot is shown in Figure 9.

If the track is subsectioned into groups of contiguous stations - 1-5 (A), 6-11 (B), 12-16 (C), and 17-21 (D), as shown in Figure 9 - a localized pattern of dependence on stability emerges. Sections A and D, and perhaps C, demonstrate the dependence of whitecaps on stability concluded by Wu (1981): that fractional coverage decreases with decreasing stability. However, the strength of that dependence is a function of location. Section C, which covers much of the warm core of the Loop, exhibits an increase in whitecaps with decreasing stability. While the entire data set lacks any kind of organization with respect to stability, the data appear to be well organized locally (within 100 km). This mesoscale variability indicates that other factors, perhaps chemical in nature, may

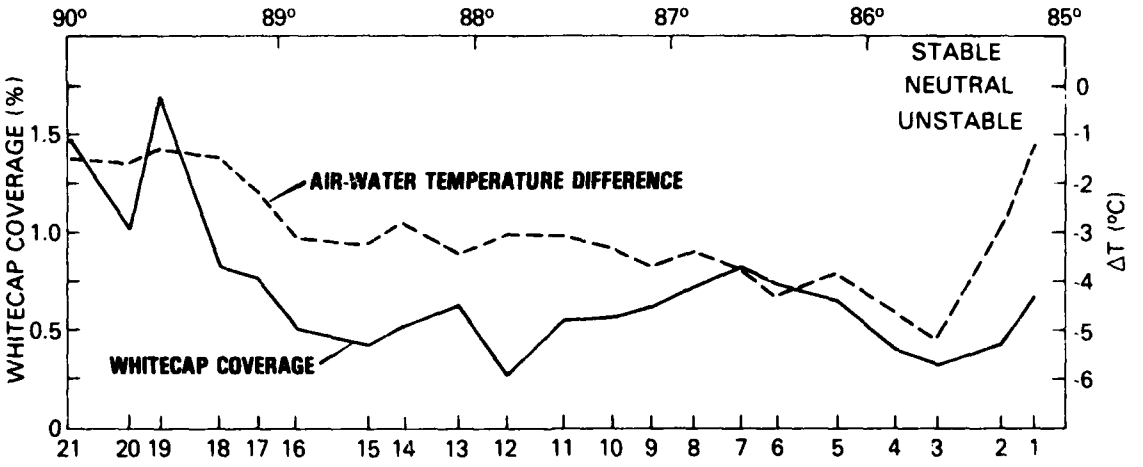

Figure 8. Coverages vs. air-sea temperature difference

affect the lifetime of the whitecap bubbles and whitecap coverage.

The fractional whitecap coverage, W, is shown plotted against mixed layer depth in Figure 10. A rough correlation exists, showing a deepening mixed layer with increased whitecap coverage that has a correlation coefficient of about 0.5. Again, much higher correlations can be achieved if the data set is partitioned as in Figure 9. Also, the locations of the two minima in coverage at 85°52'W and 87°51'W as shown in Figure 3 correlate approximately with the locations of the two mixed layer depth minima shown in Figure 5.

Conclusions

Spatial fluctuations in whitecap coverage along a 400 km stretch of ocean have been shown to be relatively insensitive to the magnitude of the local surface wind stress. Water temperature and air column stability were shown to be influential in determining bubble lifetimes and, hence, the fraction of ocean covered by foam at any instant of time. The usefulness of such information depends on the application. For example, aerosol distribution may be a strong function of the instantaneous foam coverage, whereas acoustic noise may depend more on the number of whitecaps generated per unit time per unit area.

The results of this analysis are not encouraging for the prospects of abstracting the surface wind speed from the microwave brightness of the sea surface if, as assumed, the brightness is determined in large part (for wind speed >10 m/sec) by the amount of foaming taking place on the sea surface. For example, significantly lower microwave brightness temperatures might be observed at the western Loop Current boundary than would be observed 50 km to the west. This lower temperature would be interpreted

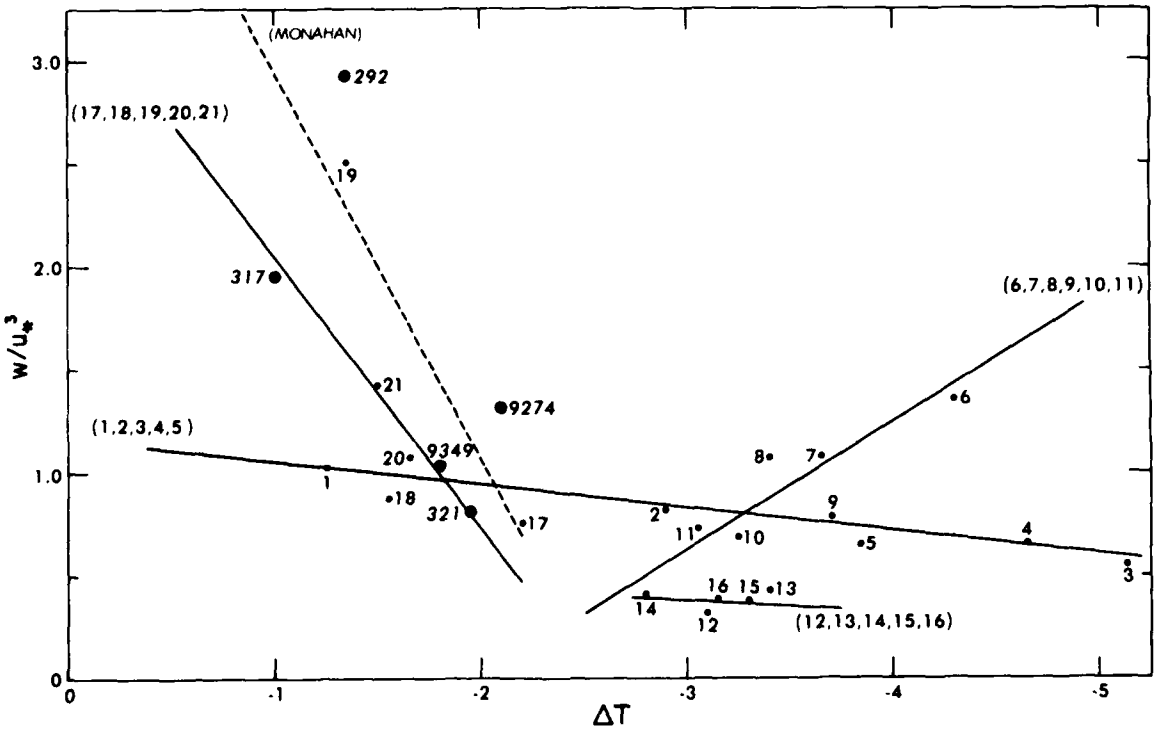

Figure 9. W/u_*^3 vs. ΔT

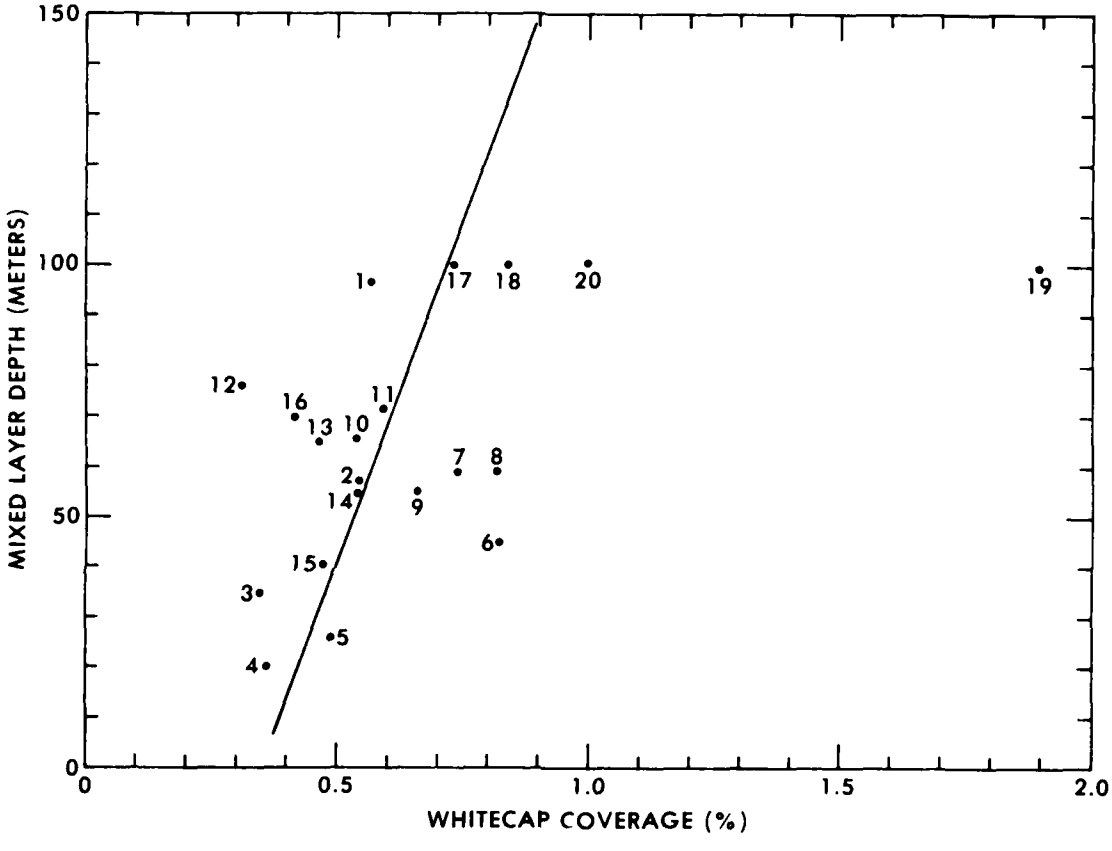

Figure 10. W vs. mixed layer depth

as indicative of a lower surface wind velocity when, in fact, the reduced brightness may have been caused by a decrease in the stability of the bubbles caused by, say, a reduction in the surfactant concentration in that area. The Loop Current, however, may represent an area of anomalous variability in the chemical and physical properties of the sea water. These conditions, coupled with the bi-directional nature of the wave field and the limited fetch of the wind, combine to provide what may likely be an atypical situation.

The results of Appendix A have shown that whitecaps are not the well-defined, sharp-edged features they appear to be. This lack of whitecap definition limits the utility of areal whitecap coverage as an independent variable in functional expressions for wind speed, wind stress, significant wave height, etc. Further research may show that some integral property of the reflectance of foam will prove to relate more closely to physical foam parameters such as bubble spectra, bubble concentration, and foam depth and, thus, relate more closely to wave dissipation rates, aerosol production, wind speed, and microwave brightness.

References

Blanchard, D. C. (1971). Whitecaps at Sea. J. Atmos. Sci., v. 28, p. 645.

Brooks, I. H. and P. P. Niiler (1977). Energetics of the Florida Current. J. Mar. Res., v. 35, p. 163.

Cardone, V.J. (1969). Specification of the Wind Distribution in the Marine Boundary Layer for Wave Forecasting. New York University Report No. TR-69-1 (AD 702490).

Cipriano, R. J. and D. C. Blanchard (1981). Bubble and Aerosol Spectra Produced by a Laboratory Breaking Wave. J. Geophys. Res. (in press).

Garrett, W. D. (1967). The Influence of Surface-Active Material on the Properties of Air Bubbles at the Air/Sea Interface. Naval Research Laboratory, Report 6545.

Longuet-Higgins, M. S., and N. D. Smith (1981). Measurements of Steep and Breaking Waves. IUCRM Symposium on Wave Dynamics and Radio Probing of the Ocean Surface.

Miyake, Y. and T. Abe (1948). Study on the Foaming of Sea Water, Part 1. J. Mar. Res., v. VII, p. 67-73.

Monahan, E. C. (1969). Laboratory Comparisons of Fresh-Water and Salt-Water Whitecaps. J. Geophys. Res., v. 74, p. 6961.

Monahan, E.C. (1971). Ocean Whitecaps. J. Phys. Oceanogr., v. 1, p. 139.

Monahan, E. C. and C. Zietlow (1969). Laboratory Comparisons of Fresh-Water and Salt-Water Whitecaps. J. Geophys. Res., v. 74, p. 6961-6966.

Ross, D. B. and V. Cardone (1974). Observations of Oceanic Whitecaps and Their Relation to Remote Measurements of Surface Wind Speed. J. Geophys. Res., v. 79, p. 444.

Toba, Y. and N. Chaen (1973). Quantitative Expression of the Breaking of Wind Waves on the Sea Surface. Rec. Oceanogr. Works, Japan, 12th, p. 1-11.

Wu, J. (1979). Oceanic Whitecaps and Sea State. J. Phys. Oceanogr., v. 9, p. 1064.

Wu, J. (1981). Bubble Populations and Spectra in Near-Surface Ocean: Summary and Review of Field Measurements. J. Geophys. Res., v. 86, p. 457.

Appendix A. Errors in the Estimation of Areal Whitecap Coverage Using Photographs

A cursory glance at the photos displayed in Figure 6 reveals that the reflection of light from foam is, by far, the strongest signal present in a photographic image of the sea surface on a sunny to partly cloudy day. It would seem an easy task (at least if one had access to an imaging computer) to measure the area of the photo that stands out from the background as whitecaps and divide by the total area to give the fractional whitecap coverage. The intensity of the image of each whitecap is not monotonic, however, but varies from a maximum value near the core of the breaker, tapering on every side down to the intensity of the background. In short, the boundary of the image of the breaker is not well-defined.

Figure A-1 is a magnified portion of one of the images used in the foregoing whitecap analysis. The whitecap in the left-center of the picture has been digitized and the intensities contoured in Figure A-2. While the center of the whitecap has limited dynamic range, the edges taper gradually in intensity from the bright core to the darker background. The cause of this variation is either a decrease in the reflectance of the whitecap as the boundaries are approached or is an artifact of the exposure process whereby the photons incident on the emulsion are of such an intensity that scattering processes within the emulsion cause a lateral diffusion of light. The degree of blooming is difficult to determine a posteriori, since no control targets were imaged during the experiment; however, Kodak specifications for 2424 film indicate that, for contrasts of 30 dB, a resolution of 80 lines per millimeter (mm) should be obtainable. As seen in Figure A-2, the lateral extent of the whitecap image on the camera backplane is 1.2 mm and, hence, describable by some 100 vertical lines. This resolution would certainly be sufficient to resolve the observed reflectance variations across the whitecap observed in Figure A-2, so we must conclude that the measured contours are representative of actual reflectance variations over the surface of the whitecap.

Whatever the source of the resulting intensity variations, the problem of estimating the boundaries remains. Several minimum intensity criteria for defining a whitecap were applied to a sample image (not the image of Figure A-1), and the resulting fractional coverage was plotted against the minimum brightness criteria for a whitecap boundary (Fig. A-3). The minimum brightness is selected from a full dynamic range of 0-256. The change in estimated coverage is shown to be quite large for a corresponding change in threshold brightness; for example, reducing the minimum brightness criteria from 160 to 155 produces a two-fold increase in apparent whitecap coverage.

Since the threshold value is arrived at quite arbitrarily (the computer analyst sets the level at whatever value seems to best define the whitecaps), whitecap coverage estimates must also be subject to a certain amount of subjectiveness. Figures A-4 and A-5 demonstrate the effect on the blotched areas of increasing the threshold from 160 to 165. These figures are enlarged whitecap images overlaid with the blotched areas for the two cases. As the threshold is raised in Figure A-5 to 165, several of the pixels from Figure A-4 no longer meet the minimum brightness criteria and are rejected, with a corresponding drop in the blotched area, and thus in the calculated areal whitecap coverage. Hence, variations in the way in which areal whitecap coverage is determined by different investigators or by the same investigator for different data sets can produce such large variations in reported whitecap coverage that intercomparisons may become meaningless. Blanchard (1971) arrived at this same

conclusion after comparing his results (Blanchard, 1963) with those of Monahan (1971).

The difficulty in judging boundaries does not, however, negate the value of comparative studies on the same data set as was done in this report. That is, if the criteria for establishing foam boundaries is kept constant together with other variables such as digitizing illumination, film type, filters, camera, shutter speed, etc., meaningful comparisons can be made.

The source of the intensity variations within each whitecap may be due to variations in bubble concentration or other properties of the bubbles. Cipriano and Blanchard (1981) measured bubble spectra at different distances from the base of a laboratory waterfall and found that the concentration of bubbles and the fraction of bubbles >300μm decreased with distance from the center of the foam. The observations described here indicate that the reflectance of foam near nadir may be a function of the shape of the bubble spectrum and/or the bubble concentration.

Obviously, not enough is known about the scattering properties of sea foam and how these properties are related to bubble spectra, bubble concentration, foam thickness, foam lifetime, etc. Further research to determine the relationship between reflectance and the physical properties of foam will determine which quantities other than areal coverage - intensity weighted coverage, for example, might be more closely related to energy dissipation or microwave emissivity.

References

Blanchard, D. C. (1971). Whitecaps at Sea. J. Atmos. Sci., v. 28, p. 645.

Blanchard, D. C. (1963). The Electrification of the Atmosphere by Particles from Bubbles in the Sea. Prog. in Oceanog., 1., p. 71-202.

Cipriano, R. J. and D. C. Blanchard (1981). Bubble and Aerosol Spectra Produced by a Laboratory Breaking Wave. J. Geophys. Res.,(in press).

Monahan, R. C. and C. Zietlow (1969). Laboratory Comparisons of Fresh-Water and Salt-water Whitecaps. J. Geophys. Res., v. 74, p. 6961-6966.

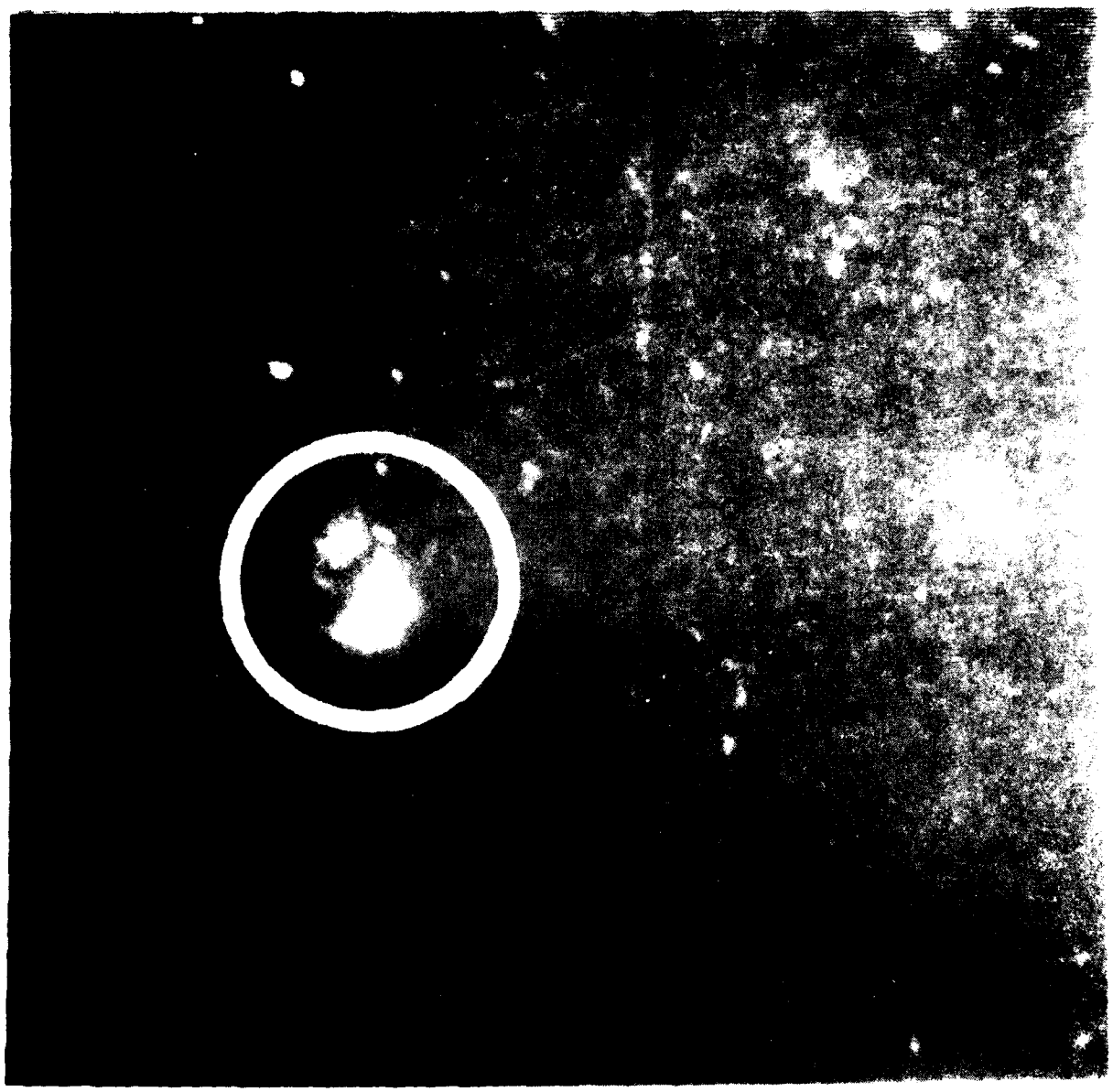

Figure A-1. Magnified sub-section of photo image of whitecap used to contour reflected light intensity

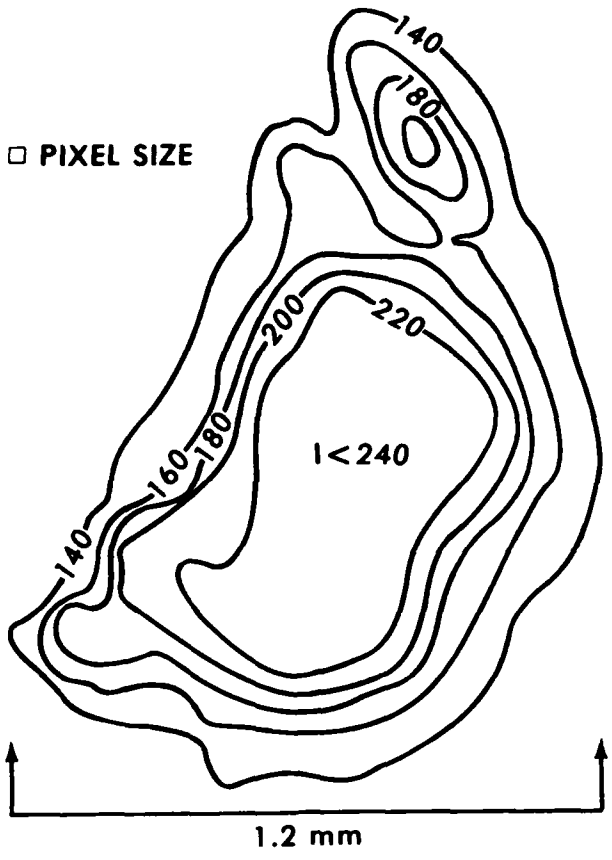

Figure A-2. Contour of the reflected light intensity from whitecap coverage for sample image

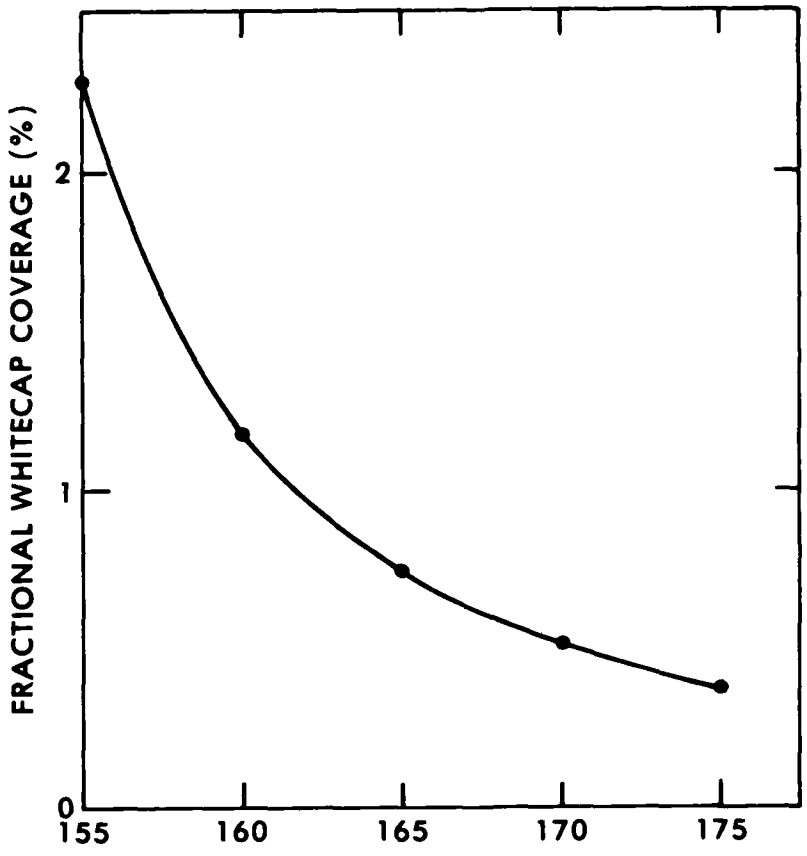

Figure A-3. Minimum brightness criteria vs. whitecap coverage for sample image

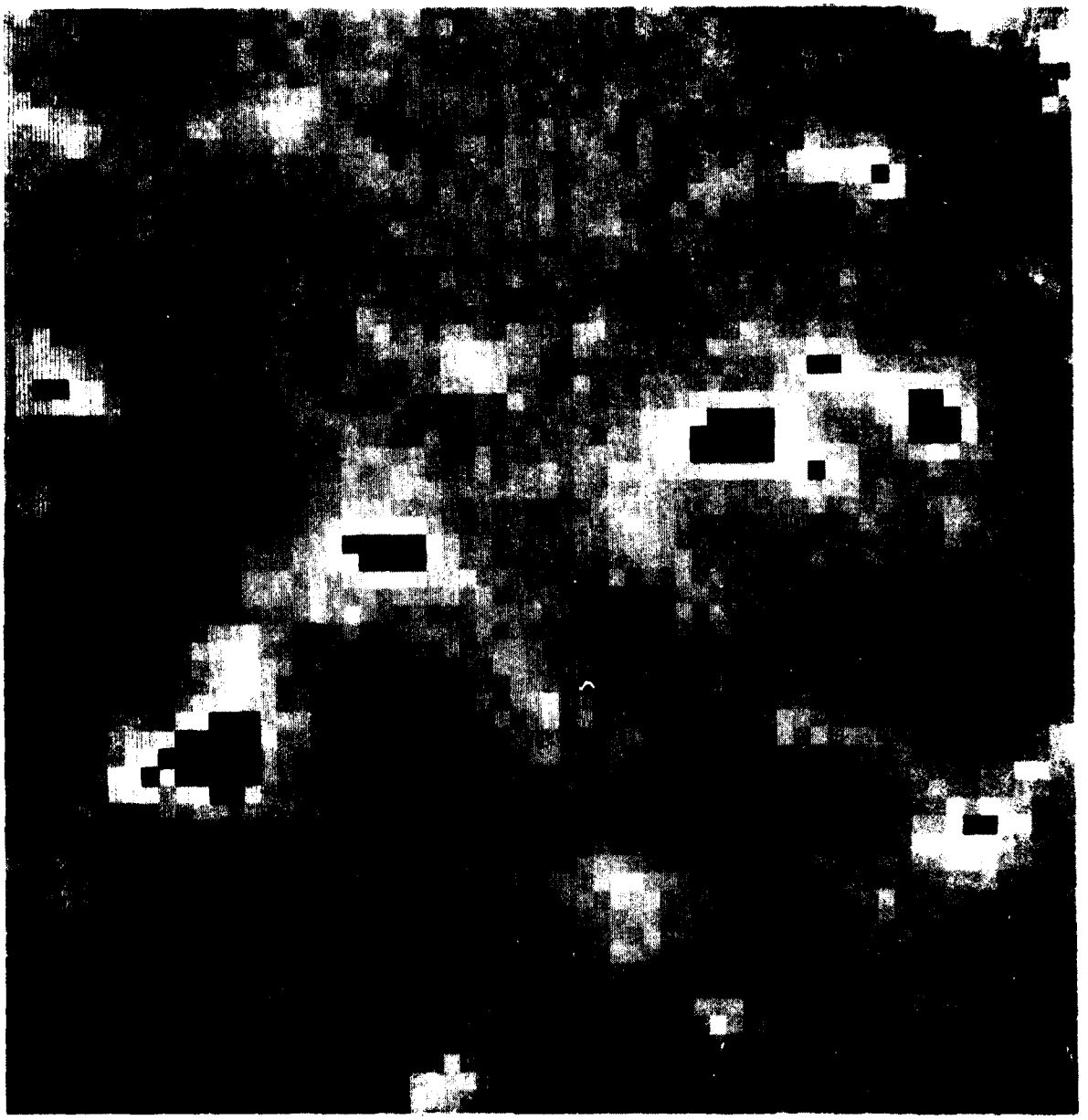

Figure A-4. Magnified, digitized image of minimum brightness set to 165

Figure A-5 Magnified digitized image of blotched whitecaps with minimum brightness set at 160

REPORT DOCUMENTATION PAGE		READ INSTRUCTIONS BEFORE COMPLETING FORM
1 REPORT NUMBER NORDA Report 43	2 GOVT ACCESSION NO.	3 RECIPIENT'S CATALOG NUMBER
4 TITLE (and Subtitle) Measurements of Whitecap Coverage and Surface Wubds Over the Gulf of Mexico Loop Current		5 TYPE OF REPORT & PERIOD COVERED 6 PERFORMING ORG. REPORT NUMBER
7 AUTHOR(s) Peter M. Smith		8 CONTRACT OR GRANT NUMBER(s)
9 PERFORMING ORGANIZATION NAME AND ADDRESS Naval Ocean Research and Development Activity NSTL Station, Mississippi 39529		10 PROGRAM ELEMENT PROJECT TASK AREA & WORK UNIT NUMBERS October 1981
11 CONTROLLING OFFICE NAME AND ADDRESS Naval Ocean Research and Development Activity NSTL Station, Mississippi 39529		12 REPORT DATE 13 NUMBER OF PAGES 24
14 MONITORING AGENCY NAME & ADDRESS (if different from Controlling Office)		15 SECURITY CLASS. (of this report) Unclassified 15a DECLASSIFICATION DOWNGRADING SCHEDULE

16 DISTRIBUTION STATEMENT (of this Report)

Distribution unlimited

17 DISTRIBUTION STATEMENT (of the abstract entered in Block 20, if different from Report)

18 SUPPLEMENTARY NOTES

19 KEY WORDS (Continue on reverse side if necessary and identify by block number)

Remote Sensing
Whitecaps
Air-Sea Interaction
Breaking Waves
Marine Boundary Layer
Loop Current
Mixed Layer

20 ABSTRACT (Continue on reverse side if necessary and identify by block number)

The fraction of the ocean surface covered by whitecaps has long been thought to be some monotonically increasing function of the prevailing wind velocity at least for large fetches. In order to determine the extent to which other factors such as air column stability or water mass type can influence the areal coverage of whitecaps, photographic data was collected over the Loop Current from a NAVOCEANO P-3 aircraft. The variation of whitecap coverage along a line of closely spaced (25 km) stations was determined and compared

with other aircraft and data buoy information. The data indicates that, on the day of the flight, white-capping within the boundaries of the Loop Current depended little on the local wind, but demonstrated a noticable dependence on air column stability. The strength and nature of this dependence varied over mesoscale distances. These results indicate that microwave radiometric measurements can be sensitive to variables other than surface wind since microwave brightness is quite sensitive to sea foam. The value of areal whitecap coverage as a measureable geophysical variable is also examined.